Design and Performance Analysis of Dual-Bands Two-Port Guitar Microstrip Patch Antenna Array for 5G Applications

Rafid A. Jasim[1] and Raed M. Shaaban[2*]

[1] Department of Physics, College of Education for Pure Science, University of Basrah, Basrah, Iraq

[2] Department of Physics, College of Science, University of Basrah, Basrah, Iraq

[*]**Corresponding author E-mail:** raed.shaaban@uobasrah.edu.iq

https://doi.org/10.29072/basjs.20260115

ARTICLE INFO

Received: 30 October 2025

Accepted: 27 January 2026

Published: 30 April 2026

Keywords:

Guitar-shaped Microstrip patch Antenna Arrays, 2x1 patch antenna array, Wideband, MIMO antenna

ABSTRACT

A guitar-shaped microstrip patch antenna with rectangular slots was developed and designed to increase bandwidth and improve gain for use in wireless communication applications such as GPS and Wi-Fi. The patch design consists of two half circle sections separated by a space containing four rectangular slots of varying lengths. These slots are arranged along the feed strip line within the second half circle, spaced 0.5 mm apart. The first half circle, with a radius of 10 mm, contains two square apertures of dimensions 2×2 mm^2 , while the second half circle, with a radius of 8 mm, contains a central rectangular aperture of 3×1.5 mm^2. The patch and ground layer have a thick of 0.035 mm. FR-4 substrate with dielectric constant 4.4 and dimension 1.55×40.3×36 mm^3, HFSS simulation software was used to design the antenna. The antenna receives and operates at two specific frequencies, 2.8 GHz and 6.8 GHz, with S_{11} reflection coefficients of -35 dB and -45 dB, respectively, demonstrating good matching and low power loss. By studying the resonant frequencies, it was found that the proposed antenna in this paper achieves gain values at 2 dB and 2.39 dB. As for the bandwidth, it was (0.5, 2.89) GHz at -10dB during the simulation process, while it was (0.43, 2.2) GHz in the experiment. The antenna efficiency is clearly shown in the C-band such as Satellite Communications, Weather Radar Systems, Wi-Fi and Cordless Phones and the X-band, such as Maritime Radar, and Air Traffic Control.

1. Introduction

Microstrip Antennas (MSA) are not just a piece of metal, but a complex science, art, and technology of communications engineering that governs the future of wireless communication and its quality in most aspect of our modern lives. In the field of wireless communications, (MSA) are essential and pivotal elements that enable the transmission and reception of information over long distances without the need for a direct physical connection between devices**[1, 2]**. In the world of communications and its applications, each antenna has specific characteristics and applications specific to that antenna. The important and very useful advantages of microstrip antennas are their light weight, small size, simple design, and low manufacturing costs**[3-5]**. Therefore, they are a favor choice in many wireless communication devices. In addition, Array antennas have the ability to precisely form beams, a feature required to increase efficiency. Microstrip antennas are not without their drawbacks, but practical solutions exist to increase efficiency and gain, as well as extend range through fabrication, feeding, and patch array geometry. Therefore, the proposed antenna represents a suitable choice for modern next-generation communication technologies, especially in smart tablets, advanced wireless communications, radar systems, medical applications, and imaging for tumor detection**[6, 7]**.In additional the array structures of microstrip antennas can be easily designed and some of their gain and efficiency characteristics can be improved**[8]**. HFSS software was used, which relies on the (FEM), one of the most accurate and comprehensive systems for analyzing complex mathematical problems in the fields of engineering, electronics, and electromagnetism in three dimensions. In conventional antennas, a single feed port is usually used. Multiple techniques are used to enhance antenna gain such as antenna array design, use of reflectors or lenses, increasing patch area, use of low-loss substrates, improving impedance matching, and use of meta-structures. Antenna arrays constitute the essential physical layer for current wireless communication, allowing careful control over radiation patterns and signal directivity via spatial beamforming**[9]**. Utilising this physical foundation, Multiple-Input Multiple-Output (MIMO) technology employs these array to capitalize on multipath propagation, markedly improving spectrum efficiency and connection stability**[10]**. A significant gap persists in the research about the interplay between array geometry and MIMO processing techniques.

Current study often overlook the bandwidth, hence constraining the practical efficiency of these systems.

In wireless communication systems, using a single antenna is much easier because it ensures one input and one output. In multi-input and multi-output (MIMO) antennas, the matter becomes more complex due to mutual interference between antennas of identical configuration. Wireless systems have greatly developed due to the exponential increase in global data traffic and the demand for ultra-reliable low–latency connectivity**[11]**. To fulfil these criteria, the shift from traditional signal-antenna systems to advanced antenna Arrays has become imperative, offering the requisite spatial degrees of freedom. These physical arrays constitute the foundation of Multiple-Input Multiple-Output(MIMO) technology, which converts multipath interference-previously a disadvantage into a strategic asset for improving spectral efficiency**[10]**. Therefore, this research proposes developing a single antenna and then converting it into a two-element array antenna, thus converting the system into a dual-element MIMO system. This allows for improving and increasing the antenna gain while maintaining antenna stability and efficiency. The proposed design maintains a high degree of structural symmetry and preserves the original single antenna structure. To maintain the basic radiation characteristics and ensure reduced structural complexity, the two MIMO elements are arranged in parallel and side by side, as shown in Figure 2b. The experimental work involved fabricating a single antenna prototype using a CNC LASER and then determining the antenna performance using a vector network analyzer (VNA). The antenna was tested in a resonance chamber to confirm the radiation characteristics. A microstrip feed line was used to excite the antenna's radiating elements with a 50 Ω impedance. To assess the performance of the MIMO antenna, important metrics like gain, bandwidth, and the dispersion coefficient(S-parameter) were computed.

2- Antenna design

2.1 Design of single port antenna

Low and medium frequency applications work best when the loss tangent value is 0.0245 and the dielectric constant is 4.4, which allows good control of the dielectric properties. At higher frequencies, some signal loss may occur. One of the insulators used in the manufacture of microstrip antennas is FR4, an insulating material with a dielectric constant of 4.4 and a thickness

of 1.55 mm. In addition to its mechanical strength, electrical stability, and market availability, this material is widely used in strip antennas and printed circuit boards. Therefore, it was used as an insulating material and a basic substrate in this design**[12]**.

One of the software tools used to simulate and design various types of antennas is the HFSS Software**[13]**. It was used to develop the proposed antenna designed in this paper. This software enables complex geometrical designs and the application of required physical conditions such as material properties (dielectric or conductive), feeding methods, and radiation limits. By studying the operating frequency, signal losses, gain, standing wave ratio (VSWR), and radiation structures, HFSS provides the ability to study and analyze antenna operation. All of this improves and develops antenna designs to achieve optimal performance for wireless communication applications. The radius of the patch can be calculated using different formulas, including**[1]**:

$$f_o = \frac{1.8412\ C}{2\pi R\sqrt{\varepsilon_r}} \qquad (\mathbf{1})$$

Where $f_o\ is$ frequencies efficiently

C is the speed of light in free-space.

And the effective radius R_e is given by

$$R_e = R_e = R\sqrt{1 + \frac{2h}{\pi R\varepsilon_r}\left\{\ln\left(\frac{\pi R}{2h}\right) + 1.7726\right\}} \qquad (\mathbf{2})$$

Therefore, the resonant frequency has to be increased as determined by equation (1) and based on equation (2) as follows.

$$f_e = \frac{1.8412\ C}{2\pi R_e\sqrt{\varepsilon_r}} = \frac{8.791\times10^9}{R_e\sqrt{\varepsilon_r}} \qquad (\mathbf{3})$$

So

$$R_e = \frac{8.791\times10^9}{f_e\sqrt{\varepsilon_r}} \qquad (\mathbf{4})$$

To achieve the optimal design for an antenna operating within the required frequency, the proposed antenna was designed in stages, including modifying the patch shape and ground plane, as follows:

The patch configuration was based on a simple circle comprising a rectangle, a strip line feeder, ground plane, and a substrate, as shown in Figure (1). For simulation purposes.

2.2 Adding structures for optimization

The circular antenna patch with a radius of 10 mm was developed by subtraction rectangle with dimensions (20, 14) mm² to form the first half circle. Followed by adding another circle

with a radius of 8 mm, followed by subtraction rectangle with dimensions (16, 12) mm² to form the second half circle patch. Inserting four slots with dimensions of (16×1), (12×1), (8×1), and (4×1) mm², with intervals of 0.5 mm between them. To achieve the optimal design shown in Figure (1), which enables the antenna to work within broadband applications. The parameters values are indicated in **Table 1**).

Table 1. The final dimensions of single element antenna

Parameter	Value (mm)	Parameter	Value (mm)	Parameter	Value (mm)	Parameter	Value (mm)
Ls	40.3	Lg	14.5	L4	12	L8	5.5
Ws	36	L1	6	L5	8	d	1.5
R1	10	L2	3	L6	16	d 1	2
R2	8	L3	4	L7	2	Lg	14.5
lf	13.3	Wf	2.3				

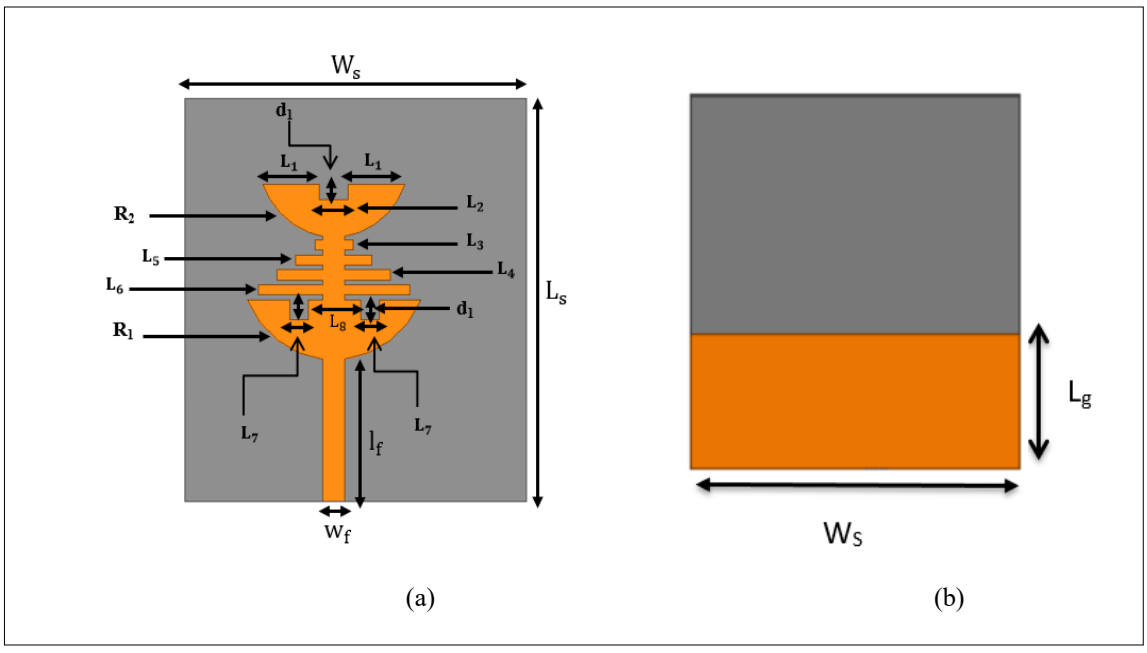

Figure 1. Structural dimensions of single port antenna(a) Top view (b) Bottom view.

3 Design of two port antenna

3.1 Antenna Array

The goal of designing a Two-port microstrip guitar patch antenna array is to achieve improved beamforming performance and increase transmission and reception efficiency. To reduce interference, control radiation direction and improve signal quality, two ports are designed on one side**[14]**. The design also aims to provide favorable radiation characteristics while increasing bandwidth and gain, making the antenna suitable for use in modern communications applications such as 5G and high-frequency (HF) networks.

Thus, this design helps improve system efficiency, provide frequency reconfiguration capability, and adapt to the requirements of diverse communications environments and millimeter wave, while reducing size and facilitating manufacturing.

Designing a two-port guitar microstrip patch antenna array includes the following steps and concepts:

3.2 Basic Patch Design:

- A linear antenna array consisting of two elements in a 2×1 arrangement and adopted as shown in Figure 2.
- The patch is the basic element in antenna design, and in this paper the shape of the patch was chosen to be inspired by the design of a guitar. The patch dimensions are chosen based on the target frequency and desired bandwidth.
- The inter-element spacing between the two antenna elements is equal to 0.67λ, where λ represents the wavelength.
- The patch is mounted on a dielectric substrate with a known dielectric constant, such as a FR4 substrate, to ensure stable performance.
- The ground plane was of a length equal to the length of the single element and of a width equal to twice the width of the element.

3.3 Two-Port Feeding:

In a two-port design, vertical and horizontal feeds are used to minimize interference between them and ensure good isolation between the two ports, as shown in Figure 2.

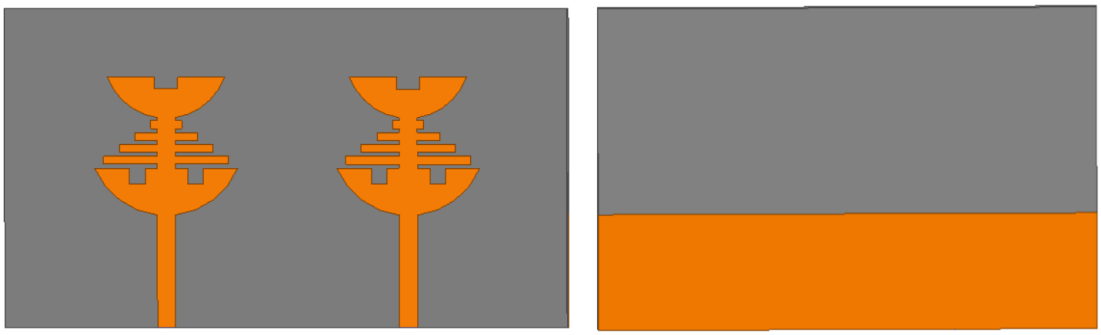

(a) (b)

Figure 2. Two-port array antenna (a) Top view (b) Bottom view.

3.4 Array Configuration of two port MIMO:

Multiple patches are arranged in an array (1x2) to maximize gain and directivity.

The Two ports feed is designed to excite the array elements with synchronous currents to achieve the desired radiation pattern.

3.5 Geometry of 2-Port MIMO antenna

The dual-port antenna was constructed using a single-element antenna setup. The substrate used to construct the antenna 40.3mm and 72mm, and the spacing between the two array elements was approximately 0.65 wavelengths. The upper side of the the antenna is shown in Figure 2a, while the lower side is shown in figure 2b. These techniques can be enhanced by increasing the separation between antenna elements or by using physical or electronic separation structures. It's worth noting that increasing the separation between elements increases the overall dimensions of the antenna, which can impact its design and overall efficiency. Improving the overall performance of the antenna is achieved by improving insulation and reducing interference between the antenna ports by preventing surface currents from traveling across the substrate surface. This is achieved by correctly connecting the grounding levels. This leads to the transmission of unwanted radiation to other system ports.**[15]**.

4 Results and discussion

4.1. S-Parameters.

The reflection coefficients S_{11} and S_{22} and the transmittance coefficients S_{12} and S_{21} were examined for both radiators in relation to one another in terms of scattering coefficients (S-parameters), as seen in Figure(3). As seen in Figure (4), the finding for S_{11} and S_{22} for two element antenna have comparable patterns, and S_{12} and S_{21} both exhibit the same behavior. Because it guarantees a predictable and controllable antenna system response, the symmetry displayed by the reflection and transmission coefficients of both two element antenna ports is desirable feature. This helps 5G applications in the rang[2-10]GHz frequency band operate better and more efficiently

(a) (b)

Figure 3. The suggested antenna setup. (a) top view and (b) bottom view.

The level of agreement between the numerical and experimental results is demonstrated by comparing the simulated and measured S11 reflection coefficient values for MIMO arrangement in Figure(5).

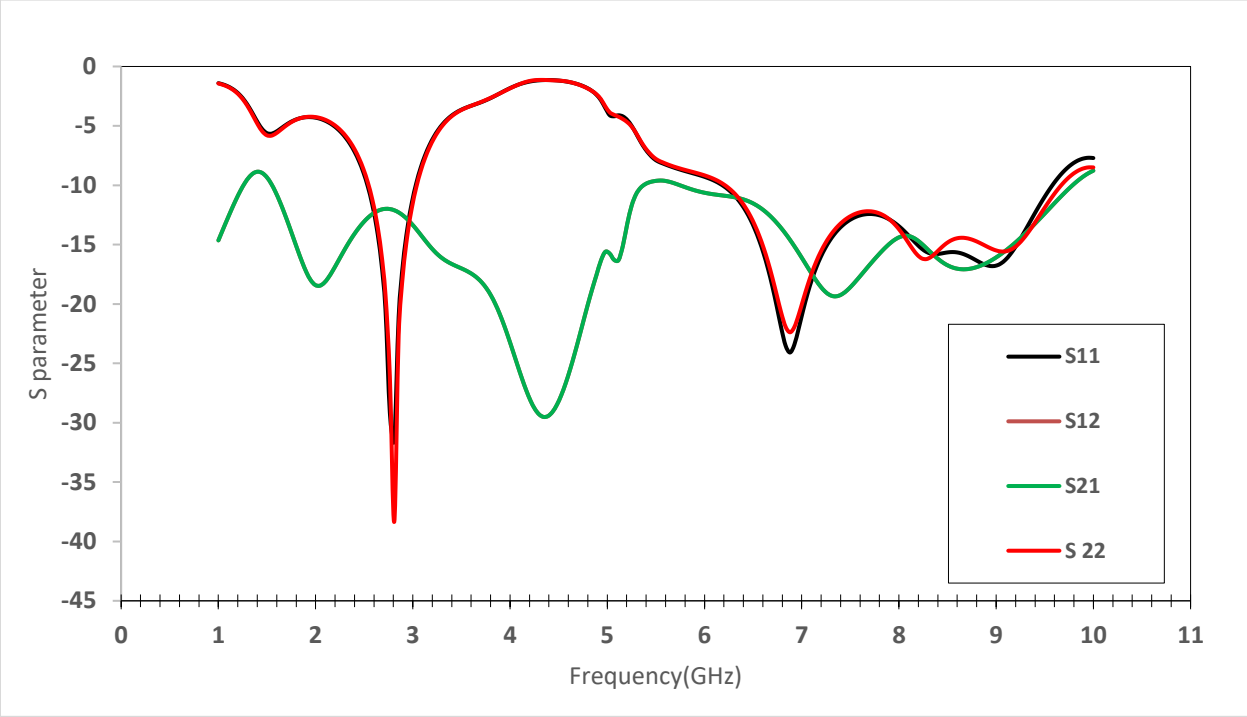

Figure 4. Suggested antenna's S-parameters.

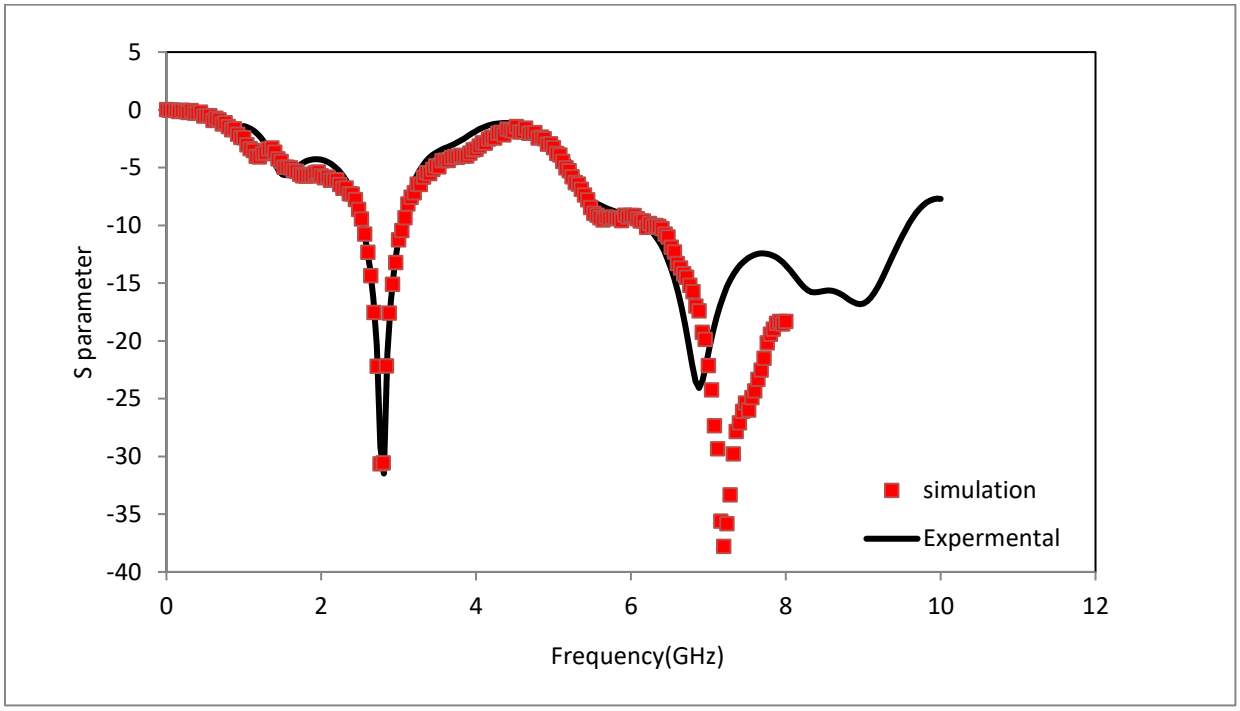

Figure 5. S11 of the proposed antenna was measured and simulated.

With a minimal reflection coefficient of -38.33 dB and -24.08dB, the antenna demonstrated a high match at the resonant frequencies of 2.8 GHz and 6.8GHz. Based on the finding of the simulated curve, the antenna offers a wide operational bandwidth of 3.39 at 6.8GHz and 0.5 at 2.8GHz, as illustrated in Figure (5).

3.2. Surface Current Distribution.

A comprehensive understanding of the consequences from the mutual coupling between antenna elements is provided by the examination of the surface current distribution in the suggested MIMO antenna. The responses that emerge in neighboring elements when one of the elements is electromagnetically activated are the main focus of this investigation. The surface current distribution for the radiator at 2.8 GHz is shown in Figure (6), with comparable responses for both ports.

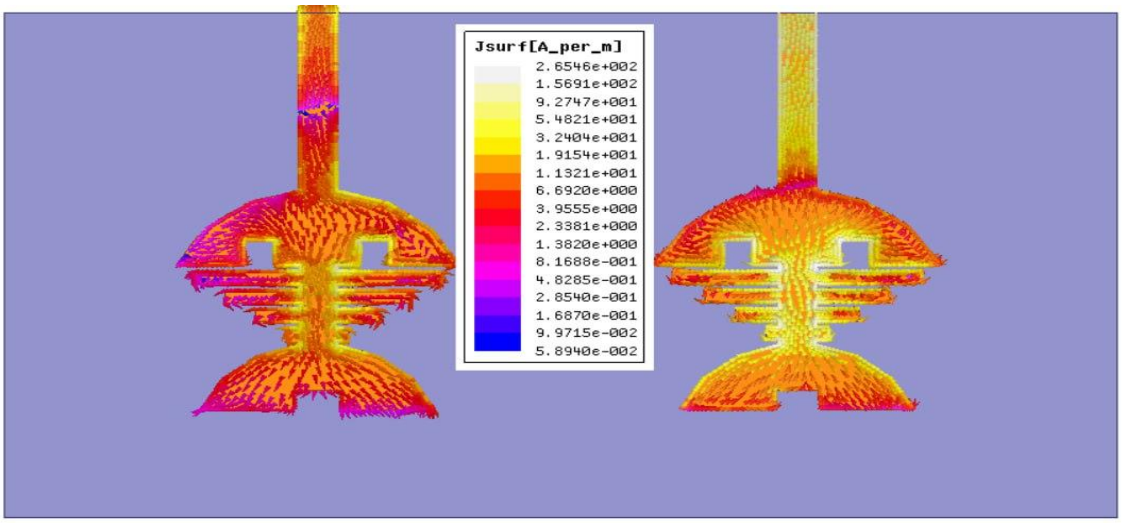

Figure 6. Simulation surface current distribution of the proposed antenna.

3.3. Radiation Patterns.

Figure (7a,b) shows the simulated and measured 2D radiation patterns at 2.8 GHz for port(1), showing both the polarized and orthogonal components in the E and H planes. The radiation pattern measurement technique, which was conducted inside an anechoic chamber to guarantee

the correctness of the results and their freedom from undesired reflections, is depicted in Figure (8). The 3D pattern of the MIMO antenna directivity at 2.8GHz for each of the two antenna ports is displayed in Figure (9 a, b). The directional radiation characteristics of the antenna are accurately seen by these patterns, which show great directivity with a limited beam width. Additionally, it is clear that both emitters concentrate the emitted energy in a broad direction, demonstrating how well the design achieves high-performance radiation characteristics.

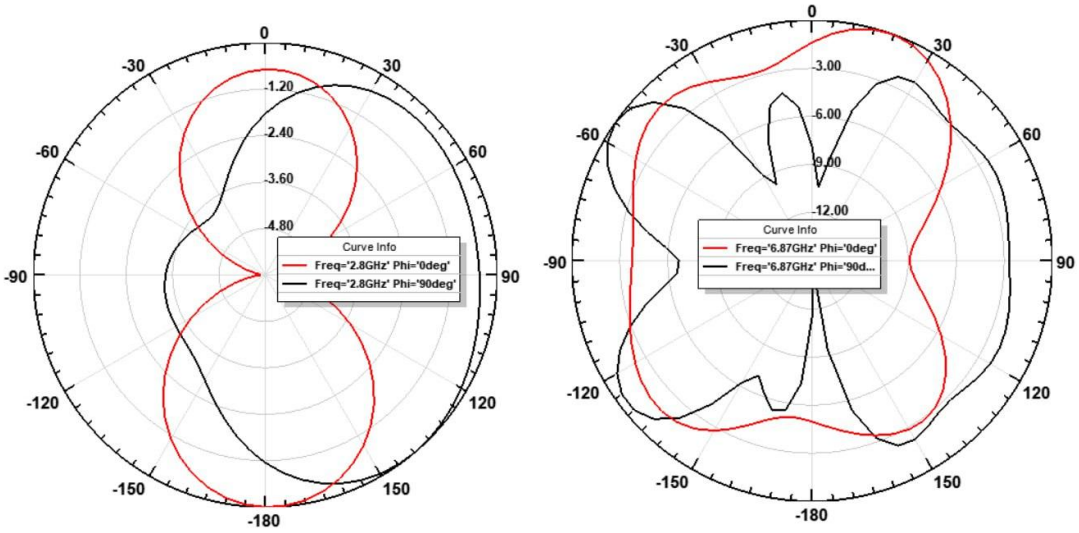

(a) (b)

Figure 7. Simulated radiation patterns (a) at 2.8GHz and (b) at 6.8 GHz of the proposed antenna.

Figure 8. Measurement setup of radiation patterns inside the anechoic chamber.

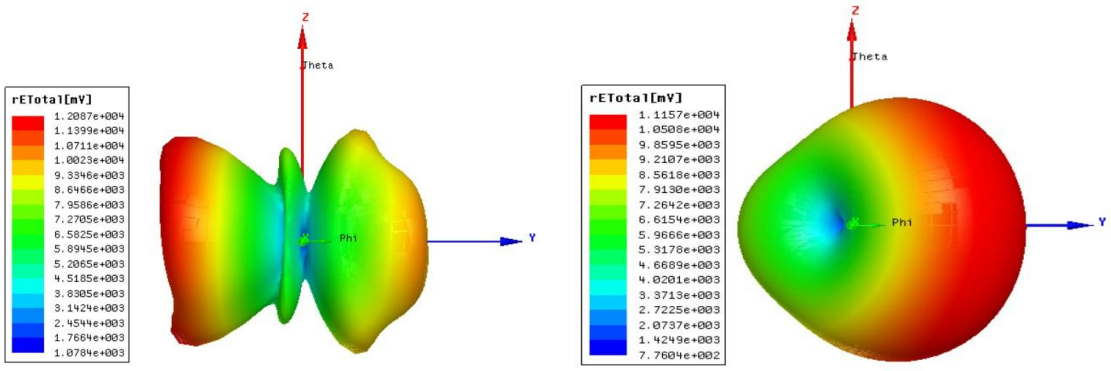

Figure 9. 3D radiation patterns for both ports of the suggested antenna with respect to directivity

3.4. Gain

As seen in Figure (10), the gain simulation results revealed a varied response over the frequency rang of 1-10GHz. High radiation performance in this range is indicated by the antenna's highest gain value of roughly 14.7dB at 3.8GHz. Additionally, the gain was found to be substantially positive over the majority of the mid – rang (4 -7GHz), with values ranging from 2-4 dB. Indicating the antenna's capacity to sustain steady radiation efficiency.

The antenna's ideal operating range was clearly defined by the declines that occurred at lower frequencies (<2 GHz) and higher frequencies (>8GHz), where the gain reached negative values up to -10 dB, Because of its exceptional mid-range performance and notable gain improvement at 3.8GHz, the suggested antenna is appropriate for wireless communication applications .

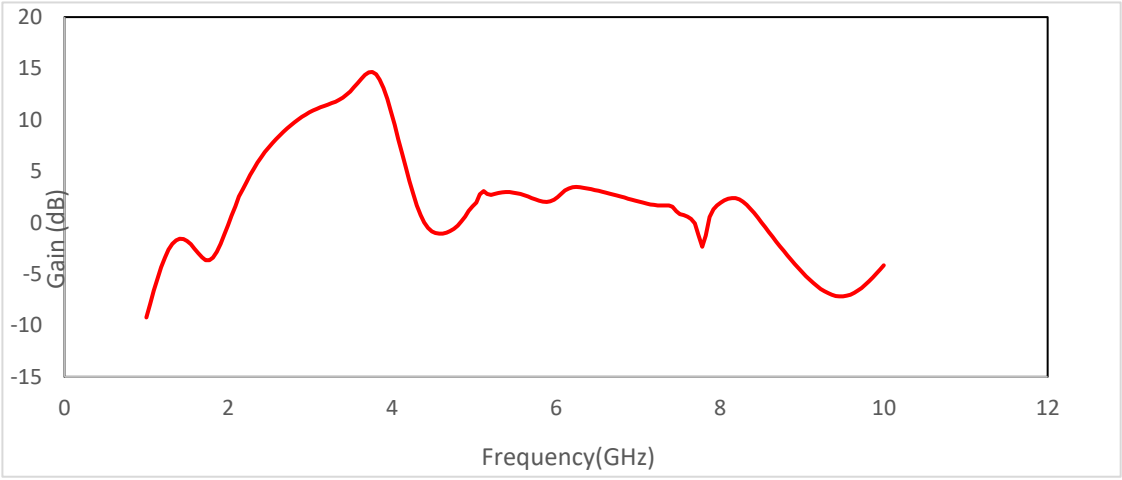

Figure 10. The suggested antenna's gain achieved.

Table 2 illustrates a comparion between the suggested design and recent academic articles, emphasizing the innovation and progress of the proposed methodology.

Table 2. Comparison of the proposed MIMO Antennas with recent latest state of the art antennas.

Ref	Antenna Type & Application	No. of Elements	Physical Dimensions (mm)	Peak Gain (dBi)	Loss Factor (Return Loss)	BW
[16]	mm-wave 5G Array (28/38 GHz)	8 (4 ports, each with a 2-element array)	25 × 20 × 0.79	10.4 at fist band (28GHz) 10.1 at second band(38GHz)	-17 dB	Dual-band: 1.61 GHz & 5.8 GHz
[17]	Spanner Shape UWB	2 elements	59.5 × 52×1.59	6.79	~ -27dB	10 GHz (2–12)GHz
[18]	Slotted Octagon 5G Sub-6 GHz (3.1–4.5 GHz)	2 elements	55 × 38 The height of the insulating substrate was	3.17	-40.8 dB	1.4 GHz (3.1–4.5) GHz
[19]	Compact Octagonal Broadband (3.7–11 GHz)	2 elements	38.64×27×0.5	6.5	-32 dB	7.3 GHz (3.7-11)GHz
[20]	Dug-hex IoT/V2V (5.9 GHz)	4 elements	50 × 50 × 1.6	7.4	-25.16 dB	755.58 MHz
[21]	Wideband planar MIMO antenna/4G, 5G Bluetooth, and WiMAX	2 elements	40×45×1.6	6	-18dB	3.73 GHz
[22]	WLAN band and satellite communication	2 elements	15.74×20×1.58	4.98227	-23dB	0.3 GHz
The suggested design	Guitar shape /2.8GHz for 5G Applications	2 elements	40.3×36×1.55	14.7	dB 38-	Dual-band: 2.53-3.5 and 6-10 GHz

4. Conclusion

The main goal of this project is creation of a 2.8 GHz MIMO antenna, makes it ideal for a variety of modern applications, including 5G applications such as microwave imaging for tumor detection and tissue monitoring. Short-rang radars used in air traffic control, navigation systems, and satellites. The start of the study is designing a single antenna operating at the same frequency while achieving wide-band performance that exhibits superior gain and bandwidth characteristics. This antenna developed resonant frequency at 2.8Ghz and has a partial ground plane. This arrangement produces an exceptional gain of 4.52 dB and an impedance bandwidth of almost 10 dB, indicating extremely effective radiation performance. The single antenna was transformed into a two element MIMO system based on this architectural foundation, which greatly enhance the antenna system's overall performance. With a notable gain enhancement of 6.46dB, the suggested MIMO system architecture exhibits exceptional wideband coverage capacity. Additional, the MIMO configuration showed a broad bandwidth between 2.53-3.5 and 6-10 GHz under -10 dB impedance condition, attaining an isolation greater than 23 dB throughout the whole operating rang and exhibiting remarkable efficiency in lowering crosstalk between components. Additionally, the MIMO antenna's measured findings completely correspond with the simulation results, demonstrating the design's uniqueness as well as its remarkable technical functions and performance features.

References:

[1] C. A. Balanis, *Antenna theory: analysis and design*, John Wiley & Sons, 2016, https://doi.621.382′4—dc222016050162.

[2] R. Barzegari, C. Ghobadi, and J. Nourinia, "A dual-band dipole array antenna with fan-beam radiation for biomedical and telecommunications applications," *Results in Engineering*, vol. 24, p. 103136, 2024, https://doi.org/10.1016/j.rineng.2024.103136.

[3] W. A. Godaymi Al-Tumah, R. M. Shaaban, and A. P. Duffy, "Design, simulation, and fabrication of a double annular ring microstrip antenna based on gaps with multiband feature," *Engineering Science and Technology, an International Journal*, vol. 29, p. 101033, 2022, https://doi.org/10.1016/j.jestch.2021.06.013.

[4] W. A. Godaymi Al-Tumah, R. M. Shaaban, A. S. Tahir, and Z. A. Ahmed, "Multi-Forked Microstrip Patch Antenna for Broadband Application," *Journal of Physics: Conference*

Series, vol. 1279, no. 1, p. 012025, Jul. 2019. https://doi.org/10.1088/1742-6596/1279/1/012025

[5] W. A. Godaymi Al-Tumah, R. M. Shaaban, and Z. A. Ahmed, "A modified E-shaped microstrip patch antenna for dual band in x- and ku-bands applications," *Journal of Physics: Conference Series*, vol. 1234, no. 1, p. 012028, Jul. 2019. https://doi.org/10.1088/1742-6596/1234/1/012028

[6] W. Y. Zhou, Y. X. Li, W. Li, M. Lu, and J. J. Xu, "A novel radiation protection method for miniaturized MIMO mobile terminal antenna design based on metamaterials," *PLoS One*, vol. 20, p. e0323299, 2025, https://doi.org/10.1371/journal.pone.0323299.

[7] W. En-naghma, M. Latrach, H. Halaq, and A. El Ougli, "An Experimental Study of a High-Gain, Wideband Circularly Polarized Printed Antenna Array at 2.45 GHz in the ISM Band for Wireless Power Transmission Applications," *Scientific African*, p. e02619, 2025, https://doi.org/10.1016/j.sciaf.2025.e02619.

[8] A. Tiwari, G. K. Soni, D. Yadav, S. V. Yadav, and M. V. Yadav, "Rectangular loaded ring shaped multiband frequency reconfigurable defected ground structure antenna for wireless communication applications," *Results in Engineering*, vol. 25, p. 104339, 2025. https://doi.org/10.1016/j.rineng.2025.104339

[9] E. Telatar, "Capacity of Multi antenna Gaussian Channels," Lucent Technologies, Bell Laboratories, 1999, https://doi.org/10.1002/ett.4460100604.

[10] G. J. Foschini and M. J. Gans, "On limits of wireless communications in a fading environment when using multiple antennas," *Wireless Personal Communications*, vol. 6, pp. 311-335, 1998, https://doi.org/10.1023/A:1008889222784.

[11] J. G. Andrews, S. Buzzi, W. Choi, S. V. Hanly, A. Lozano, A. C. Soong, and J. C. Zhang, "What will 5G be?," *IEEE Journal on Selected Areas in Communications*, vol. 32, pp. 1065-1082, 2014, https://doi.org/10.1109/JSAC.2014.2328098.

[12] D. H. Hashim and W. A. G. Al-Tumah, "Optimize the performance of slotted circular patch antenna by using triangular slots for C-Band applications and simulation it using HFSS," vol. 2899, p. 070006, 2023, https://doi.org/10.1063/5.0172034.

[13] S. Merino-Fernandez, J. Del Pino, and S. Khemchandani, "Design of rectangular patch antennas through machine learning," *Scientific Reports*, vol. 15, p. 33605, 2025. https://doi.org/10.1038/s41598-025-18939-2

[14] Y. Wang, X. He, J. Wang, S. Berezin, and W. Mathis, "Antenna Array Pattern Synthesis via Coordinate Descent Method," *Journal of Electromagnetic Analysis and Applications*, vol. 07, pp. 168-177, 2015, https://doi.org/10.15488/1524.

[15] H. V. Singh, D. V. S. Prasad, and S. Tripathi, "Self-isolated MIMO antenna using mixed coupling by close coupling technique," *Scientific Reports*, vol. 13, p. 5636, 2023, https://doi.org/10.1038/s41598-023-32364-3.

[16] M. Mahaboob Basha, P. Pradeep, S. Gundala, and J. Syed, "Design of compact and high gain dual-band four-port MIMO antenna array for mm-wave 5G Communications," *Results in Engineering*, vol. 25, p. 104153, 2025, https://doi.org/10.1016/j.rineng.2025.104153.

[17] V. Satam, S. Nema, and S. S. Thakur, "Spanner shape monopole MIMO antenna with high gain for UWB applications," in *Proceedings of International Conference on Wireless Communication: ICWiCom 2017*, 2018, pp. 129-138, https://doi.org/10.1007/978-981-10-8339-6_15.

[18] N. Agrawal, M. Gupta, and S. Chouhan, "Modified ground and slotted MIMO antennas for 5G sub-6 GHz frequency bands," *International Journal of Microwave and Wireless Technologies*, vol. 15, pp. 817-825, 2023, https://doi.org/10.1017/S1759078722000770.

[19] R. Dhananjeyan, S. Ramesh, D. R. Kumar, and O. P. Kumar, "Compact octagonal MIMO antenna system for broadband applications with enhanced isolation and wideband performance," *Scientific Reports*, vol. 15, p. 18921, 2025, https://doi.org/10.1038/s41598-025-03494-7.

[20] H. Troudi, C. Baccouch, B. Chibani, A. Zouinkhi, A. Flah, C. Z. El-Bayeh, and K. Al-Haddad, "Integration of frequency selective surfaces with MIMO antennas for enhanced performance in IoT and V2V communication systems," *Scientific Reports*, vol. 15, p. 35545, 2025. https://doi.org/10.1038/s41598-025-19483-9

[21] D. Tadesse, O. P. Acharya, and S. Sahu, "Wideband MIMO antenna mutual coupling reduction with electromagnetic band-gap structure," *IETE Journal of Research*, vol. 69, pp. 6014-6021, 2023, https://doi.org/10.1080/03772063.2021.1984321.

[22] K. Ghosh, M. Pratap, R. Kumar, and S. Pratap, "Mutual coupling reduction of microstrip MIMO antenna using microstrip resonator," *Wireless Personal Communications*, vol. 112, pp. 2047-2056, 2020, https://doi.org/10.1007/s11277-020-07138-z.

تصميم وتحليل أداء مصفوفة هوائيات رقعة ميكروستريب كيتار الشكل ثنائية النطاق ثنائية المنافذ لتطبيقات الجيل الخامس

[1] رافد عمارجاسم و [2] رائد مسلم شعبان

[1] قسم الفيزياء, كلية التربية للعلوم الصرفة, جامعة البصرة , البصرة , العراق.

[2] قسم الفيزياء, كلية العلوم , جامعة البصرة , البصرة, العراق.

المستخلص

تم تطوير وتصميم هوائي رقعي دقيق على شكل غيتار بفتحات مستطيلة لزيادة عرض النطاق الترددي وتحسين الكسب لاستخدامه في تطبيقات الاتصالات اللاسلكية مثل نظام تحديد المواقع العالمي (GPS)وشبكة الواي فاي Wi-Fi. يتكون تصميم الهوائي من نصفي دائريين يفصل بينهما فراغ يحتوي على أربع فتحات مستطيلة بأطوال مختلفة. رُتبت هذه الفتحات على طول خط التغذية داخل النصف الدائري الثاني بمسافة 0.5 مم بينها. النصف الدائري الأول يكون بنصف قطر 10 ملم، ويحتوي على فتحتين مربعتين بأبعاد 2×2 ملم^2، بينما النصف الدائري الثاني يكون بنصف قطر 8 ملم يحتوي على فتحة مستطيلة مركزية بأبعاد 3×1.5 ملم^2. يبلغ سمك طبقة الهوائي والطبقة الأرضية 0.035 ملم. تم استخدام ركيزة FR-4 ذات ثابت عزل كهربائي 4.4 وأبعاد 1.55×40.3×36 ملم^3، وتم تصميم الهوائي باستخدام برنامج المحاكاة .HFSSيستقبل الهوائي ويعمل بترددين محددين، 2.8 جيجاهرتز و6.8 جيجاهرتز، بمعاملات انعكاس S11 تبلغ -35 ديسيبل و-45 ديسيبل على التوالي، مما يدل على توافق جيد وفقد منخفض للطاقة. وبدراسة ترددات الرنين، وُجد أن الهوائي المقترح في هذه الورقة يحقق قيم كسب تبلغ 2 ديسيبل و2.39 ديسيبل. أما بالنسبة لعرض النطاق الترددي، فقد كان (0.5، 2.89) جيجاهرتز عند -10 ديسيبل خلال عملية المحاكاة، بينما كان (0.43، 2.2) جيجاهرتز في التجربة. وتتجلى كفاءة الهوائي بوضوح في النطاق C، مثل اتصالات الأقمار الصناعية، وأنظمة رادار الطقس، وشبكات الواي فاي، والهواتف اللاسلكية، وفي النطاق X، مثل الرادار البحري، ومراقبة الحركة الجوية.

الكلمات المفتاحية: مصفوفات هوائيات رقعية دقيقة على شكل غيتار، مصفوفة هوائيات رقعية 1x2، نطاق ترددي واسع، هوائي MIMO.